Protecting a quantum memory for a photonic polarization qubit in a cold atomic ensemble by dynamical decoupling

Yuelong Wu, Lirong Chen, Zhongxiao Xu, and Hai Wang*

The State Key Laboratory of Quantum Optics and Quantum Optics Devices, Institute of Opto-Electronics, Shanxi University, Taiyuan, 030006, China

*wanghai@sxu.edu.cn

Abstract: We report an experimental demonstration of storage of photonic polarization qubit (PPQ) protected by dynamical decoupling (DD). PPQ's states are stored as a superposition of two spin waves by electromagnetically-induced-transparency (EIT). Carr-Purcell-Meiboom-Gill (CPMG) DD sequences are applied to the spin-wave superposition to suppress its decoherence. Thus, the quantum process fidelity remains better than 0.8 for up to 800μs storage time, which is 3.4-times longer than the corresponding storage time of ~180μs without the CPMG sequences. This work is a key step towards the storage of single-photon polarization qubit protected by the CPMG sequences.

©2014 Optical Society of America

OCIS codes: (270.5585) Quantum information and processing; (140.3550) Lasers, Raman; (020.3320) Laser cooling; (020.7010) Laser trapping.

References and links

1. L. M. Duan, M. D. Lukin, J. I. Cirac, and P. Zoller, "Long-distance quantum communication with atomic ensembles and linear optics," Nature **414**(6862), 413–418 (2001).
2. P. Kok, W. J. Munro, K. Nemoto, T. C. Ralph, J. P. Dowling, and G. J. Milburn, "Linear optical quantum computing with photonic qubits," Rev. Mod. Phys. **79**(1), 135–174 (2007).
3. A. I. Lvovsky, B. C. Sanders, and W. Tittel, "Optical quantum memory," Nat. Photon. **3**(12), 706–714 (2009).
4. Z. B. Chen, B. Zhao, Y. A. Chen, J. Schmiedmayer, and J. W. Pan, "Fault-tolerant quantum repeater with atomic ensembles and linear optics," Phys. Rev. A **76**(2), 022329 (2007).
5. J. W. Pan, Z. B. Chen, C. Y. Lu, H. Weinfurter, A. Zeilinger, and M. Zukowski, "Multi-photon entanglement and interferometry," Rev. Mod. Phys. **84**(2), 777–838 (2012).
6. M. Fleischhauer and M. D. Lukin, "Dark-state polaritons in electromagnetically induced transparency," Phys. Rev. Lett. **84**(22), 5094–5097 (2000).
7. T. Chanelière, D. N. Matsukevich, S. D. Jenkins, S. Y. Lan, T. A. B. Kennedy, and A. Kuzmich, "Storage and retrieval of single photons transmitted between remote quantum memories," Nature **438**(7069), 833–836 (2005).
8. L. Karpa, F. Vewinger, and M. Weitz, "Resonance beating of light stored using atomic spinor polaritons," Phys. Rev. Lett. **101**(17), 170406 (2008).
9. S. Riedl, M. Lettner, C. Vo, S. Baur, G. Rempe, and S. Dürr, "Bose-Einstein Condensate as a quantum memory for a photonic polarization qubit," Phys. Rev. A **85**(2), 022318 (2012).
10. B. Zhao, Y. A. Chen, X. H. Bao, T. Strassel, C. S. Chuu, X. M. Jin, J. Schmiedmayer, Z. S. Yuan, S. Chen, and J. W. Pan, "A millisecond quantum memory for scalable quantum networks," Nat. Phys. **5**(2), 95–99 (2009).
11. R. Zhao, Y. O. Dudin, S. D. Jenkins, C. J. Campbell, D. N. Matsukevich, T. A. B. Kennedy, and A. Kuzmich, "Long-lived quantum memory," Nat. Phys. **5**(2), 100–104 (2009).
12. Y. O. Dudin, S. D. Jenkins, R. Zhao, D. N. Matsukevich, A. Kuzmich, and T. A. B. Kennedy, "Entanglement of a photon and an optical lattice spin wave," Phys. Rev. Lett. **103**(2), 020505 (2009).
13. Z. Xu, Y. Wu, L. Tian, L. Chen, Z. Zhang, Z. Yan, S. Li, H. Wang, C. Xie, and K. Peng, "Long lifetime and high-fidelity quantum memory of photonic polarization qubit by lifting zeeman degeneracy," Phys. Rev. Lett. **111**(24), 240503 (2013).
14. Y. O. Dudin, A. G. Radnaev, R. Zhao, J. Z. Blumoff, T. A. B. Kennedy, and A. Kuzmich, "Entanglement of light-shift compensated atomic spin waves with telecom light," Phys. Rev. Lett. **105**(26), 260502 (2010).
15. D. J. Szwer, S. C. Webster, A. M. Steane, and D. M. Lucas, "Keeping a single qubit alive by experimental dynamic decoupling," J. Phys. At. Mol. Opt. Phys. **44**(2), 025501 (2011).
16. S. Yu, P. Xu, X. He, M. Liu, J. Wang, and M. Zhan, "Suppressing phase decoherence of a single atom qubit with Carr-Purcell-Meiboom-Gill sequence," Opt. Express **21**(26), 32130–32140 (2013).
17. G. de Lange, Z. H. Wang, D. Ristè, V. V. Dobrovitski, and R. Hanson, "Universal dynamical decoupling of a single solid-state spin from a spin bath," Science **330**(6000), 60–63 (2010).

#216479 - $15.00 USD Received 7 Jul 2014; revised 17 Aug 2014; accepted 1 Sep 2014; published 17 Sep 2014

18. J. Du, X. Rong, N. Zhao, Y. Wang, J. Yang, and R. B. Liu, "Preserving electron spin coherence in solids by optimal dynamical decoupling," Nature **461**(7268), 1265–1268 (2009).
19. F. Jelezko, T. Gaebel, I. Popa, M. Domhan, A. Gruber, and J. Wrachtrup, "Observation of coherent oscillation of a single nuclear spin and realization of a two-qubit conditional quantum gate," Phys. Rev. Lett. **93**(13), 130501 (2004).
20. Y. O. Dudin, L. Li, and A. Kuzmich, "Light storage on the time scale of a minute," Phys. Rev. A **87**(3), 031801 (2013).
21. M. Lovrić, D. Suter, A. Ferrier, and P. Goldner, "Faithful solid state optical memory with dynamically decoupled spin wave storage," Phys. Rev. Lett. **111**(2), 020503 (2013).
22. G. Heinze, C. Hubrich, and T. Halfmann, "Stopped light and image storage by electromagnetically induced transparency up to the regime of one minute," Phys. Rev. Lett. **111**(3), 033601 (2013).
23. M. Fleischhauer and M. D. Lukin, "Quantum memory for photons: dark-state polaritons," Phys. Rev. A **65**(2), 022314 (2002).
24. Z. Xu, Y. Wu, H. Liu, S. Li, and H. Wang, "Fast manipulation of spin-wave excitations in an atomic ensemble," Phys. Rev. A **88**(1), 013423 (2013).
25. T. Yuge, S. Sasaki, and Y. Hirayama, "Measurement of the noise spectrum using a multiple-pulse sequence," Phys. Rev. Lett. **107**(17), 170504 (2011).
26. M. A. Nielsen, "A simple formula for the average gate fidelity of a quantum dynamical operation," Phys. Lett. A **303**(4), 249–252 (2002).
27. J. Bylander, S. Gustavsson, F. Yan, F. Yoshihara, K. Harrabi, G. Fitch, D. G. Cory, Y. Nakamura, J. S. Tsai, and W. D. Oliver, "Noise spectroscopy through dynamical decoupling with a superconducting flux qubit," Nat. Phys. **7**(7), 565–570 (2011).
28. Y. W. Cho and Y. H. Kim, "Atomic vapor quantum memory for a photonic polarization qubit," Opt. Express **18**(25), 25786–25793 (2010).
29. D. G. England, P. S. Michelberger, T. F. M. Champion, K. F. Reim, K. C. Lee, M. R. Sprague, X. M. Jin, N. K. Langford, W. S. Kolthammer, J. Nunn, and I. A. Walmsley, "High-fidelity polarization storage in a gigahertz bandwidth quantum memory," J. Phys. At. Mol. Opt. Phys. **45**(12), 124008 (2012).
30. R. Loudon, *The Quantum Theory of Light* (Oxford University, 2004).
31. X. H. Bao, X. F. Xu, C. M. Li, Z. S. Yuan, C. Y. Lu, and J. W. Pan, "Quantum teleportation between remote atomic-ensemble quantum memories," Proc. Natl. Acad. Sci. U.S.A. **109**(50), 20347–20351 (2012).

1. Introduction

Photons with their polarization states encoding in quantum information are good for transmitting quantum information. For realizing long-distance quantum communication [1] and scalable quantum computing [2], long-lived quantum memories for a photonic polarization qubit are crucial [3–5]. Many physical processes have been exploited to store quantum states of light. The absorptive electromagnetically-induced-transparency [6] and emissive spontaneous-Raman-emission processes [1] in atomic ensembles provide promising storage schemes. In both schemes, photonic states are stored as spin waves and then retrieved after a demand time. However, due to decoherence, the spin waves will decay with time and will be only effectively retrieved within storage lifetimes. There are several factors that limit the lifetimes of quantum memories in atomic ensembles. For the storages of a certain polarization state of light, only a single spin wave is required and the decoherence for such storages includes two main factors: atomic motion and inhomogeneous Zeeman broadening. For storages of photonic polarization qubit (PPQ), two spin waves (SWs) [7,8] are required. Thus, besides the above-mentioned two decoherence mechanisms, random phase between the two SWs caused by magnetic field fluctuations will degrade polarization fidelity and then lead to decoherence [9]. In the past several years, many studies on suppressions of spin-wave decoherence have been done and several methods have been proved to be effective. The decoherence resulting from atomic motion can be significantly suppressed by using cold atoms in magneto-optical traps [10] or ultra-cold atoms in optical lattice [11] as storage media and the decoherence caused by spatial gradient of magnetic fields and their temporal fluctuations can be obviously decreased by storing PPQ's states as two magnetic-field-insensitive coherences [12,13] or two spatially distinct SWs [14] associated with the clock coherence. Another method to suppress the random phase in PPQ's storages is to compensate the magnetic field noise by using an open-loop feed-forward technique [9]. In the past few years, a powerful strategy, known as dynamical decoupling (DD) technique, has been developed to protect qubit memories in single atoms [15,16], array of ions [17], spin ensembles [18], NV-center systems [19] and so on. In very recent years [20–22], the optical quantum storages based on electromagnetically induced transparency (EIT) has also been

#216479 - $15.00 USD Received 7 Jul 2014; revised 17 Aug 2014; accepted 1 Sep 2014; published 17 Sep 2014
(C) 2014 OSA

introduced. By applying DD sequences to rotate the two states of a spin wave, the longest storage lifetimes for a fixed polarization light are 16 seconds in atoms confined in optical lattice [20] and 1 minute in solid-state ensembles [22]. However, the experiments of suppressing random phase between the two spin waves in the PPQ's storages by DD have not been demonstrated.

In this paper, we experimentally demonstrate the PPQ's storages protected by Carr-Purcell-Meiboom-Gill (CPMG) DD pulse sequences. Based on EIT effect in a cold atomic ensemble, the PPQ is stored as two spin waves, which are associated with the magnetic-field-insensitive and magnetic-field-sensitive coherences, respectively. The CPMG sequences containing multiple Raman π pulses are applied to suppress decoherence of the spin waves and thus the quantum process fidelity remains better than 0.8 for up to 800μs storage time.

2. Theoretical discussion for protecting PPQ's storage by CPMG DD sequences

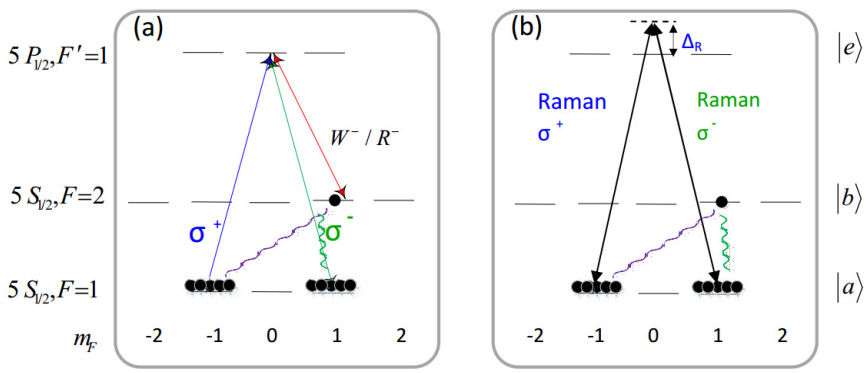

Fig. 1. The atomic level schemes of ^{87}Rb for EIT storages (a) and Raman π rotations (b), respectively. σ^+ and σ^+ are the right- and left-circularly-polarized signal fields, respectively. W^- / R^- is the left-circularly-polarized writing/reading field. Δ_R denotes the detuning of the Raman laser from the transition $|a\rangle \leftrightarrow |e\rangle$.

The involved levels of ^{87}Rb atoms are shown in Fig. 1(a) and 1(b), where $|a\rangle = |5^2S_{1/2}, F=1\rangle$, $|b\rangle = |5^2S_{1/2}, F=2\rangle$ and $|e\rangle = |5^2P_{1/2}, F'=1\rangle$. All of the atoms are prepared in an incoherent mixture of the $|a_{m_F=\pm1}\rangle$ states (m_F denotes the magnetic quantum number) with equal population. The signal and writing/reading light fields propagate along *z*-axis, whose frequencies are tuned to transitions $|a\rangle \leftrightarrow |e\rangle$ and $|b\rangle \leftrightarrow |e\rangle$, respectively, and their frequency difference equals to the frequency ω_{ab} of the transition $|a\rangle \leftrightarrow |b\rangle$. The writing/reading light field is left circular polarization and the input signal-light field is an arbitrary polarization state. The signal-light field can be written as

$$\vec{\varepsilon}(t) = \vec{\varepsilon}_R(t) + \vec{\varepsilon}_L(t) = |\vec{\varepsilon}(t)|\left(\alpha|R\rangle + \beta e^{i\varphi}|L\rangle\right), \tag{1}$$

where $\vec{\varepsilon}_R(t)$ and $\vec{\varepsilon}_L(t)$ denote the right-circularly (σ^+) and left-circularly (σ^-) polarized components, respectively, $|R\rangle$ and $|L\rangle$ are their unit vectors, $|\vec{\varepsilon}(t)| = \sqrt{|\varepsilon_R(t)|^2 + |\varepsilon_L(t)|^2}$, $\alpha = |\vec{\varepsilon}_R(t)| / |\vec{\varepsilon}(t)|$ and $\beta = |\vec{\varepsilon}_L(t)| / |\vec{\varepsilon}(t)|$. The Stokes parameters [9] of the input signal field can be written as:

#216479 - $15.00 USD Received 7 Jul 2014; revised 17 Aug 2014; accepted 1 Sep 2014; published 17 Sep 2014
(C) 2014 OSA

$$\begin{pmatrix} S_0^{in} \\ S_1^{in} \\ S_2^{in} \\ S_3^{in} \end{pmatrix} = \left|\vec{\varepsilon}(t)\right|^2 \begin{pmatrix} 1 \\ 2\alpha\beta\sin\theta \\ \alpha^2-\beta^2 \\ 2\alpha\beta\cos\theta \end{pmatrix} \tag{2}$$

The quantum axis defined by a bias magnetic field B_z is along z-direction, so, the $\sigma^{\pm}$- polarized components of the signal field couple to $\left|a_{m_F=-1}\right\rangle \leftrightarrow \left|e_{m_F=0}\right\rangle$ and $\left|a_{m_F=1}\right\rangle \leftrightarrow \left|e_{m_F=0}\right\rangle$ transitions, respectively, and the σ^--polarized writing/reading light field couples $\left|b_{m_F=1}\right\rangle \leftrightarrow \left|e_{m_F=0}\right\rangle$ transition. These couplings form two three-level Λ-type EIT systems: $\left|a_{m_F=\pm1}\right\rangle - \left|e_{m_F=0}\right\rangle - \left|b_{m_F=1}\right\rangle$. The spin waves $\hat{S}_+$ and $\hat{S}_-$, which associate with the magnetic-field-insensitive coherence $\left|a_{m_F=-1}\right\rangle \leftrightarrow \left|b_{m_F=1}\right\rangle$ and magnetic-field-sensitive coherence $\left|a_{m_F=1}\right\rangle \leftrightarrow \left|b_{m_F=1}\right\rangle$, respectively, are defined by [23],

$$\hat{S}_{\pm}(z,t) = \left(N_z\right)^{-1} \sum_{z_j \in N_z} \left|a_{m_F=\pm1}\right\rangle_{jj} \left\langle b_{m_F'=1}\right| e^{i\omega_{ab}t}, \tag{3}$$

where, $N_z = Ndz/l$ is the number of atoms between z and $z+dz$, l is the length of the atomic ensemble. The conversion between the arbitrarily polarized signal-light fields and the two spin waves are described by the theory of two dark-state polaritons [24]. According to the theory, the σ^+- and σ^-- polarized signal light fields will be converted into spin waves $\hat{S}_-$ and $\hat{S}_+$, respectively, if the writing beam is turned off over a very short time interval $\left[t_0,\ t_1\right]$. Such conversion will create a superposition:

$$\vec{S}(z,t_1) = \hat{S}_-(z,t_1) + \hat{S}_+(z,t_1) = \left|\vec{S}(z,t_1)\right|\left(\alpha\vec{s}_+ + \beta e^{-i\varphi}\vec{s}_-\right). \tag{4}$$

where, $\left|\vec{S}(z,t_1)\right| = \sqrt{\left|\vec{S}_+(z,t_1)\right|^2 + \left|\vec{S}_-(z,t_1)\right|^2}$, $\vec{s}_+$ and $\vec{s}_-$ are spin-wave unit vectors and defined by: $\vec{s}_+ = \hat{S}_+(z,t_1)/\left|\hat{S}_+(z,t_1)\right|$ and $\vec{s}_- = \hat{S}_-(z,t_1)/\left|\hat{S}_-(z,t_1)\right|$. During the storage time, the spin waves $\hat{S}_+$ and $\hat{S}_-$ will suffer from decoherence and undergo Larmor processes, respectively. For the presented storage scheme, the time interval $t_1 - t_0$ is close to zero, so we have $t_0 \approx t_1$. Assuming $t_0 = 0$, the superposition at time t will evolve into:

$$\vec{S}(z,t) = \left|\hat{S}(z,0)\right| e^{-t/2\tau_d - i\omega_{ab}t}\left(\alpha e^{-t/2\tau_+ - i\Omega_+ t - i\int_0^t \omega_+(t)dt'}\vec{s}_+ + e^{i\varphi}\beta\vec{s}_- e^{-t/2\tau_- - i\Omega_- t - i\int_0^t \omega_-(t)dt'}\right), \tag{5}$$

where, τ_d is the lifetime limited by atomic motions, $\tau_{\pm}$ are the lifetimes for the magnetic-field-sensitive and magnetic-field-insensitive spin waves $\hat{S}_+$ and $\hat{S}_-$, respectively, which are limited by inhomogeneous Zeeman broadening [11], $\Omega_{\pm} = -\frac{\mu_B B_{z0}}{\hbar}\left(g_b \pm g_a\right)$ ($\omega_{\pm} = -\frac{\mu_B \delta B_z}{\hbar}\left(g_b \pm g_a\right)$) are the Larmor frequencies for the transitions $\left|a_{m_F=\pm1}\right\rangle \leftrightarrow \left|b_{m_F=1}\right\rangle$, which are induced by the guiding magnetic field B_{z0} (fluctuations of magnetic field $\delta B_z(t)$)

#216479 - $15.00 USD Received 7 Jul 2014; revised 17 Aug 2014; accepted 1 Sep 2014; published 17 Sep 2014
(C) 2014 OSA

along z axis, $g_a \approx 0.5018$, $g_b \approx 0.4998$ are the Landé factors. If the reading beam is switched on at this time t, the spin-wave supposition will be transferred into the retrieved light field according to [24]:

$$\vec{\varepsilon}^{out}(t) = \sqrt{R}\vec{S}(z,t) \propto \sqrt{R}e^{-t/2\tau_d - i\omega_{ab}t}\left(\alpha e^{-t/2\tau_+}\left|R\right\rangle + e^{i\varphi}\beta e^{-t/2\tau_- - i\Omega t - i\int_0^t \delta_\omega(t)dt'}\left|L\right\rangle\right), \quad (6)$$

where, R is the retrieval efficiency, $\Omega = \left(\Omega_- - \Omega_+\right) = 2g_a \frac{\mu_B}{\hbar} B_z$ ($\delta_\omega(t) = \left(\delta\omega_-(t) - \delta\omega_+(t)\right) = 2g_a \frac{\mu_B}{\hbar}\delta B_z(t)$) is the difference of Larmor frequency between the SWs S_+ and S_-, which are induced by guiding magnetic field B_z (magnetic field noise $\delta B_z(t)$). The calculated Stokes parameters for the retrieved light field are:

$$\begin{pmatrix} S_0^{out} \\ S_1^{out} \\ S_2^{out} \\ S_3^{out} \end{pmatrix} = R\,\mathrm{e}^{-t/\tau_d}\begin{pmatrix} \alpha^2 e^{-t/\tau_+} + \beta^2 e^{-t/\tau_-} \\ 2\alpha\beta e^{-t(1/2\tau_+ + 1/2\tau_-)}W(t)\sin(\Omega t + \varphi) \\ \alpha^2 e^{-t/\tau_+} - \beta^2 e^{-t/\tau_-} \\ 2\alpha\beta e^{-t(1/2\tau_+ + 1/2\tau_-)}W(t)\cos(\Omega t + \varphi) \end{pmatrix}, \quad (7)$$

where, $W(t) = \exp\left\langle\left[-\int_0^t \delta_\omega(t')dt'\right]\right\rangle = \exp\left[-\int_0^\infty \frac{d\omega}{2\pi}S(\omega)\left|f_0(\omega)\right|^2\right]$ is the normalized coherence [25], $S(\omega) = \int_{-\infty}^{\infty} dt e^{i\omega t}\left\langle\delta_\omega(t)\delta_\omega(0)\right\rangle$ is noise spectrum, $f_0(t,\omega) = \int_0^t dt' e^{i\omega t'}$. If t is large enough, we have

$$W(t) = \mathrm{e}^{-t/T_0}, \quad (8)$$

where $T_0 = 1/S(0)$ is the coherence lifetime [26]. The quantum state fidelity is defined by

$$F_{st} = Tr\left(\rho_{in}\rho_{out}\right). \quad (9)$$

where, $\rho_{in(out)} = \frac{1}{2}\sum_{i=0}^{3}\frac{S_i^{in(out)}}{S_0}\hat{\sigma}_i$ are the input (output) density matrices, $\hat{\sigma}_i$ are the Pauli spin operator. We calculate the quantum state fidelities for six input states based on the Eqs. (7)–(9), the results are:

$$F_{st(X)} \approx \frac{1}{2} + \frac{e^{-t(1/2\tau_+ + 1/2\tau_-)}W(t)\cos\Omega t}{e^{-t/\tau_+} + e^{-t/\tau_-}}, \quad (10)$$

for $\left|X\right\rangle = \left|H\right\rangle, \left|V\right\rangle, \left|A\right\rangle, \left|D\right\rangle$ and

$$F_{st(X)} = 1, \quad (11)$$

for $\left|X\right\rangle = \left|R\right\rangle, \left|L\right\rangle$, where H, V, R, L, D and A denote horizontal, vertical, right circular, left circular, diagonal (45°), and antidiagonal (–45°) polarizations, respectively. The quantum process fidelity can be expressed as [26]:

$$F_p \approx \frac{3\overline{F_{\mathrm{st}}} - 1}{2}, \quad (12)$$

#216479 - $15.00 USD Received 7 Jul 2014; revised 17 Aug 2014; accepted 1 Sep 2014; published 17 Sep 2014
(C) 2014 OSA

where $\bar{F}_{st} = (F_{st(H)} + F_{st(V)} + F_{st(A)} + F_{st(D)} + F_{st(R)} + F_{st(L)})/6$ is the average quantum state fidelity. Based on Eqs. (10)–(12), we calculate the quantum process fidelity, the result is:

$$F_{st(X)} \approx \frac{1}{2} + \frac{e^{-t(1/2\tau_+ + 1/2\tau_-)} W(t) \cos \Omega t}{e^{-t/\tau_+} + e^{-t/\tau_-}}, \tag{13}$$

where, $\theta = \Omega t$ is the relative phase between the SWs $\hat{S}_+$ and $\hat{S}_-$. According to the above equation, we may find that two factors cause decoherence of the qubit memory and make quantum process fidelity decrease with time. One factor is magnetic-field fluctuations, which causes a random phase between two spin waves and then makes the normalized coherence $W(t)$ exponentially decay with the storage time. Another is difference between the lifetimes τ_+ and τ_-, which also degrade the quantum process fidelity after a storage time *t*. The relative phase $\theta = \Omega t$ changes with the storage time, which will lead to an oscillation of process fidelity F_p. However, it can be compensated by using linear optical elements or selecting the reading times at $t_j = j\Delta T$ (where j is an integer and $\Delta T = 2\pi / \Omega$ is the time interval) to make $\theta = 2j\pi$. In this case, $\cos\theta = 1$ can be remained and the oscillation of process fidelity will be avoided. When the storage time is very long, $W(t) \to 0$ and the quantum process fidelity F_p will be close to the boundary of $\frac{1}{2}$. Such boundary corresponds to the case where the retrieval signal is unpolarized light when the input signal is a linearly-polarized light.

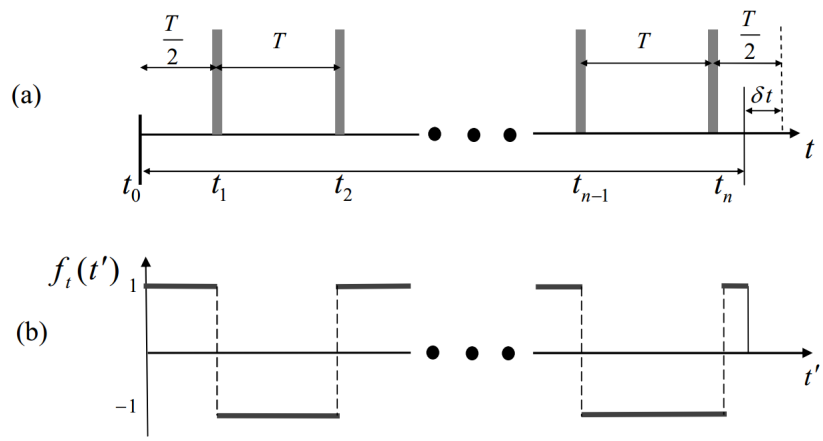

Fig. 2. (a) CPMG π pulse sequence. (b) The illustration of function $f(t')$ (*n*: even).

For suppressing decoherence caused by the two factors, we can apply CPMG DD sequences to decouple the spin-wave superposition from environment noise. The CPMG sequences contains n instantaneous π pulses applied at times t_1, t_2, …, t_n, with time delays: $t_1 - t_0 = T/2$, $t_{k+1} - t_k = T$ (as shown in Fig. 2(a)), its frequency is $F_{dd} = \frac{1}{T/2}$. Assuming that each π pulse is ideal (means that it doesn't cause any spin-wave decay), it can swap spin waves in a superposition according to:

$$\alpha\vec{s}_- + \beta e^{-i\varphi}\vec{s}_+ \to \alpha\vec{s}_+ + \beta e^{-i\varphi}\vec{s}_-. \tag{14}$$

#216479 - $15.00 USD Received 7 Jul 2014; revised 17 Aug 2014; accepted 1 Sep 2014; published 17 Sep 2014
(C) 2014 OSA

Such swapping can be viewed as a π rotation of the spin-wave superposition. Considering the case where the number of the π-pulses applied within the storage time t is even, i.e., $n = 2m$ (m is an integer), the evolution of the superposition $S(z,t)$ for $t \in [t_{n=2m},\ t_{n=2m+1}]$ is:

$$\begin{aligned}\vec{S}(z,t) &= \hat{S}_+(z,t) + \hat{S}_-(z,t) \\ &= \left|\vec{S}(z,t_0)\right| H(t)\left(\alpha e^{-\frac{\delta t}{2\tau_+}}\vec{s}_+ + e^{i\varphi}\beta W(\tau) e^{-\frac{\delta t}{2\tau_-} - i\Omega\delta t - i\int_\tau^{\tau+\delta t}\delta_\omega(t)dt}\vec{s}_-\right),\end{aligned} \tag{15}$$

where, $H(t) = e^{-t/2\tau_d - i(\omega_0+\delta\omega_+)\tau - (1/2\tau_+ + 1/2\tau_-)\tau/2}$, $\delta t = t - \tau$ with a range of $\left[-\frac{T}{2}, \frac{T}{2}\right]$, $\tau = t_{2m} + T/2$, the normalized coherence $W(\tau) = \exp\left[-\int_0^\infty \frac{d\omega}{2\pi} S(\omega)\left|f_n(\omega,\ \tau)\right|^2\right]$, $S(\omega) = \int_{-\infty}^{\infty} dt e^{i\omega t}\left\langle \Delta(t)\Delta(0)\right\rangle$, $f_n(\omega,\tau) = \int_{-\infty}^{\infty} dt' e^{i\omega t'} f(t')$, $f(t')$ is given by:

$$f(t') = 0 \text{ for } t' < 0 \text{ or } t' > \tau \ ,$$
$$f(t') = (-1)^l \text{ for } t_k < t' < t_{k+1}, k = 0, 1, 2, 3 \ldots 2m \ .$$

when $\tau \to \infty$, the normalized coherence $W(\tau) \to e^{-\frac{2S(\pi/2T)}{\pi^2}\tau}$ [25]. Since the magnetic-field fluctuation $\delta B_z(t)$ is a typical $1/f^\alpha$-type noise [27], so its power spectrum $\lim_{\omega\to\infty} S(\omega) \to 0$. If the DD period T is short enough, we have $S(\pi/2T) \to 0$ and $W(t) \to 1$. Also, the short period T leads to $\delta t \to 0$ i.e., $e^{-\frac{\delta t}{2\tau_\pm}} \to 1$ and $e^{-i\int_\tau^{\tau+\delta t}\delta_\omega(t)dt} \to 1$. In this case, the two factors causing decoherence are eliminated and spin-wave superposition is changed into:

$$S(z,t) = \left|\vec{S}(z,t_0)\right| H(t)\left(\alpha\vec{s}_+(z,t) + \beta e^{-i\varphi - i\Omega\delta t}\vec{s}_-(z,t)\right). \tag{16}$$

According to the Eq. (15), we derive the quantum process fidelity:

$$F_p \approx \frac{1+\cos\vartheta}{2}. \tag{17}$$

where $\vartheta = \Omega\delta t$ is the relative phase, which may cause an oscillation of quantum process fidelity with the time interval δt . Similar to the above discussion for θ , we may take $\cos\vartheta = 1$ by compensating the relative phase or selecting appropriate retrieval times. In this case, quantum process fidelity $F_p \to 1$, which means that the CPMG DD sequences may effectively suppress the two decoherence factors.

If the number of the π-pulses applied within the storage time t is odd ($n = 2m-1$) and the period T is short enough, the time evolution of the superposition at time $t \in [t_{n=2m-1},\ t_{n=2m}]$ can be written as:

$$S(z,t) = \left|\vec{S}(z,t_0)\right| H(t)\left(\alpha\vec{s}_-(z,t) + \beta e^{-i\varphi - i\vartheta}\vec{s}_+(z,t)\right), \tag{18}$$

where $\tau = t_{2m-1} + T/2$. Comparing with the superposition manipulated by $2m$ π pulses (See Eq. (15)), we find that this is a swapped superposition. For correcting this superposition, we have to apply an additional π-pulse to it after (2m-1)-th π-pulse and then it will be changed into the one that is the same with Eq. (15).

#216479 - $15.00 USD Received 7 Jul 2014; revised 17 Aug 2014; accepted 1 Sep 2014; published 17 Sep 2014
(C) 2014 OSA

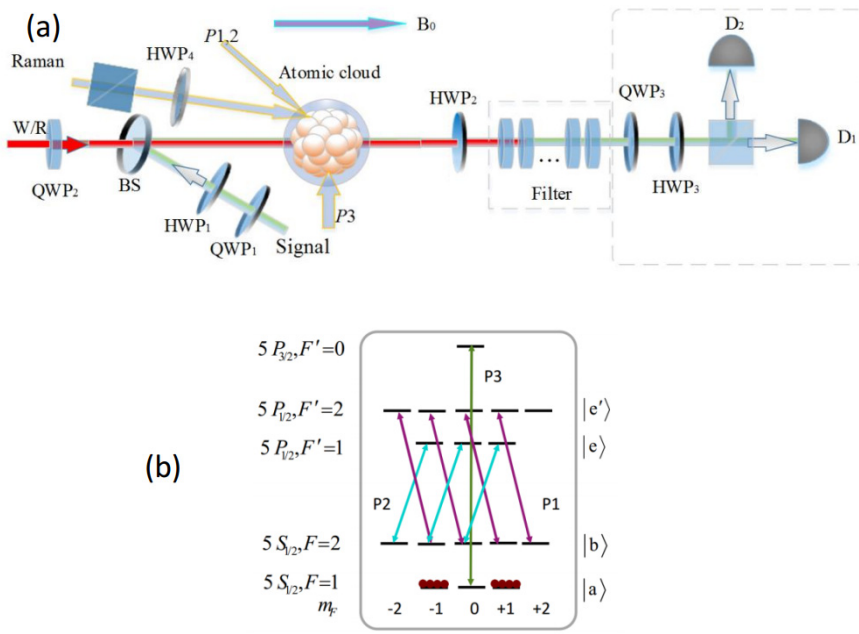

Fig. 3. (a) The experimental setup. HWP: half-wave plate; QWP: quarter-wave plate; PBS: polarizing beam splitter; BS: polarization-insensitive beam splitter; $D_{1,2}$: Photon detectors. (b) The involved atomic level scheme of ^{87}Rb for optical pumping.

3. Experimental set-up and results

The experimental setup is shown in Fig. 3 (a). A cold ^{87}Rb atomic cloud in a magneto-optical trap serves as the memory medium. A polarization-insensitive beam-splitter (BS) is used to combine the input signal and writing/reading light beams. Before arriving BS, the signal beam goes through a quarter-wave plate (QWP_1) and a half-wave plate (HWP_1). By adjusting QWP_1 and HWP_1, the polarization state of the signal light can be arbitrarily set. For suppressing the dephasing effect resulting from atomic motion, we make the signal and writing/reading light beams collinearly go through the cold-atom cloud along *z*-direction. The powers (diameters) of the writing-reading and signal beam are 3mW (2mm) and 34μW (1mm), respectively. The horizontally-polarized Raman laser beam (with a ~4.5mm diameter) passes through the cold atoms with a deviation angle of ~0.2° from $\hat{z}$. It is tuned to the transitions $|a\rangle \leftrightarrow |e\rangle$ with a blue detuning $\Delta_R = 90MHz$ (see Fig. 1 (b)). We use an analogue acousto-optic modulator (AOM) to modulate Raman laser amplitude and then obtain a rectangular pulse with a time length of 150ns. By carefully set the input power of the Raman laser beam, we realize a π-rotation between the SW $\hat{S}_+$ and $\hat{S}_-$. As shown in Fig. 3(b), the σ^-- polarized pumping laser *P*1 and σ^+- polarized pumping laser *P*2 collinearly propagate through the atoms with a deviation angle ~2° from *z*-direction, which drive the transitions $\left|5^2S_{1/2}, F=2, m_F\right\rangle \leftrightarrow \left|5^2P_{1/2}, F'=2, m_F\text{-}1\right\rangle$ and $\left|5^2S_{1/2}, F=2, m_F\right\rangle \leftrightarrow \left|5^2P_{1/2}, F'=1, m_F+1\right\rangle$, respectively. The π-polarized pumping laser *P*3 propagates through the atoms along *x*-direction, which drives the transition $\left|5S_{1/2}, F=1, m_F=0\right\rangle \leftrightarrow \left|5^2P_{3/2}, F'=0, m_F=0\right\rangle$. The powers and diameters of the lasers *P*1, *P*2 in the center of cold atoms are approximately equal, which are ~10 mW and ~7 mm, respectively, while that of the laser *P*3 is ~400 μW and ~8.8 mm, respectively. For each experimental circle, the durations for the preparation of the cold atoms and storage-retrieval experiments are ~98 ms and 2 ms, respectively. During the

#216479 - $15.00 USD Received 7 Jul 2014; revised 17 Aug 2014; accepted 1 Sep 2014; published 17 Sep 2014
(C) 2014 OSA

preparation stage, ^{87}Rb atoms are loaded into magneto-optical trap (MOT) and then performed a Sisyphus cooling. The evaluated magneto-optical trap temperature is ~200 μK, the number of the atoms in the MOT $n_a \approx 1\times10^9$, optical density is ~ 4, size of the cloud $V \approx 64mm^3$. After the Sisyphus cooling we apply a dc magnetic field $B_0 = 375\text{mG}s$ along $\hat{z}$ to define the quantization axis. Then the pump P1, 2, 3 as well as the writing laser beams are switched on to prepare the atoms into the desired ground state $\left|a_{m_F=1}\right\rangle$ or $\left|a_{m_F=-1}\right\rangle$ with the same population. After about 20μs, the pump P1, 2, 3 are turned off and the signal pulse (with a pulse length of 200ns) is injected into the atom ensemble. At the falling edge of the signal pulse (corresponding to $t_0 = 0$), the writing laser beam is ramped to zero and thus the signal pulse is mapped into the spin-wave superposition $S(z,t_0)$. We then apply CPMG pulse sequences to manipulate the spin waves. By switching on the reading light beam, we retrieve optical signals from the spin waves. Since the reading and retrieval signal beams will propagate collinearly along z-axis, we have to block the reading beam by using a set of filters [13]. Then only the retrieved signals enter a polarization analyzing and measuring (PAM) system. The PAM system consists of a quarter-wave plate (QWP_3), a half-wave plate (HWP_3), a Glan-laser polarizer (GLP) and detectors $D_{1,2}$ (Hamamatsu C5331). With QWP_2 and HWP_3, we can select the polarization basis $H-V$, $L-R$ or $D-A$ in turn for the polarization analyzing and measuring.

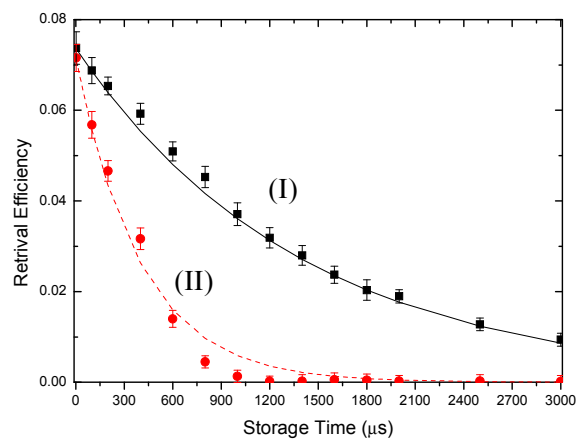

Fig. 4. The retrieval efficiencies as the function of the storage time. The square dots in curve (I) and circle dots in curve (II) are the measured results for σ^+ -polarized and σ^- -polarized fields, respectively.

We first measure the retrieval efficiencies as the function of time t. The square (black) and circle (red) dots in Fig. 4 are the measured results for (I) σ^+ -polarized and (II) σ^- -polarized fields, respectively. The solid (black) and dash (red) curves are the fits to these data based on $Re^{-t/\tau}$, yielding $1/e$ lifetimes of $\tau_+ = 1.4ms$ for magnetic-field-insensitive SW $\hat{S}_+$ and $\tau_- = 0.47ms$ for the magnetic-field-sensitive SW $\hat{S}_-$.

#216479 - $15.00 USD Received 7 Jul 2014; revised 17 Aug 2014; accepted 1 Sep 2014; published 17 Sep 2014
(C) 2014 OSA

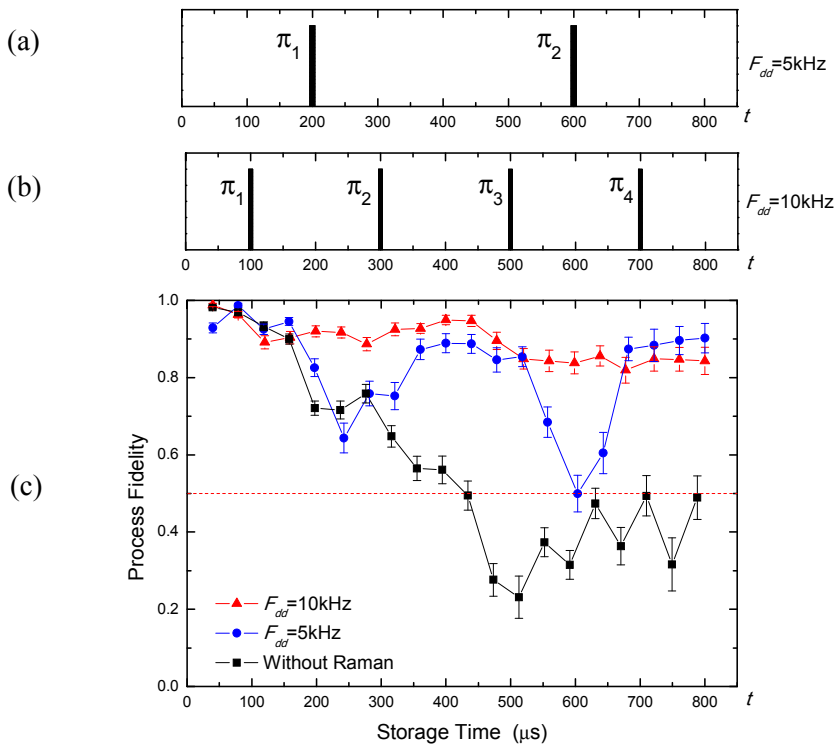

Fig. 5. (a) and (b) The applied CPMG sequences for $F_{dd} = 5kHz$ and $F_{dd} = 10kHz$, respectively. π_i ($i = 1,2,3,4$) is the i-th π pulse. (c) The quantum process fidelities F_p as the function of the storage time. The square dots are the results without the CPMG sequence. The circle and triangle dots are the results with CPMG sequences of 5-kHz and 10-kHz frequencies, respectively. The horizontal dashed (red) line is the boundary of 1/2.

We next perform the storage and retrieval of $|H\rangle$, $|V\rangle$, $|D\rangle$ and $|R\rangle$ polarization light with and without CPMG pulse sequences, respectively. Figures 5(a) and 5(b) illustrate the π-pulse sequences for $F_{dd} = 5kHz$ and $F_{dd} = 10kHz$, respectively. Based on the polarized analysis for the measured data of retrieval signals, we reconstruct the density matrix ρ_{out} and then obtain quantum process fidelities. Figure 5(c) shows the quantum process fidelities as the function of the storage time. According to the measured Larmor frequency difference Ω, we determine the time interval ΔT and then select reading at times of $t_j = j\Delta T$ (For details see Sec.2). In Fig. 5(c), the square dots correspond to the results when CPMG pulse sequence is not applied. It shows that the quantum process fidelity reduces to ~80% at 180μs. At $t \approx 500\mu s$, the quantum process fidelity reaches ~25%, which is less than the boundary of 1/2. We attribute this to inaccurate determination of the time interval ΔT. The circle and triangle dots are quantum process fidelities when CPMG pulse sequences with frequencies of $F_{dd} = 5kHz$ and $F_{dd} = 10kHz$ are applied, respectively. In the measurements for the two cases, if the stored optical signals are retrieved after (2m-1)-th π pulse, we apply an additional π-pulse to correct the spin-wave superposition before the retrieval of the optical signals. For $F_{dd} = 5kHz$, two dips appear around $t = 200\mu s$ and $t = 600\mu s$, respectively. While, for $F_{dd} = 10kHz$, the quantum process fidelity keeps a monotonous decrease with the storage time. The reason for this is explained in the following. As discussed in Sec.2, the main

#216479 - $15.00 USD Received 7 Jul 2014; revised 17 Aug 2014; accepted 1 Sep 2014; published 17 Sep 2014
(C) 2014 OSA

decoherence factors in the presented storage system are the magnetic field fluctuation δB_z and the difference between the lifetimes τ_+ for the spin wave (SW) $\hat{S}_+$ and τ_- for the SW $\hat{S}_-$. Both the two factors make the quantum process fidelity degrade with the storage time *t*. In the case where the CPMG pulse sequences are not applied, the quantum process fidelity keeps a monotonous decrease with the storage time *t*. However, at storage time $t < 100\mu s$, the decrease of the quantum process fidelity caused by the two decoherence factors is not significantly since the time interval is short. While, the decrease of the quantum process fidelity will become significant at $t \geq 200\mu s$. In the case where a CPMG π-pulse sequence with $F_{dd} = 5kHz$ is applied, the first π-pulse is applied at $t = 200\mu s$. Thus, after $t = 200\mu s$ the quantum process fidelity increases with *t* since the two spin waves have been swapped. At time $t = 400\mu s$, it is the end of a spin-echo time interval, the quantum process fidelity recovers a larger value. At $400\mu s < t < 800\mu s$, the quantum process fidelity experiences an evolution process similar to that in $200\mu s < t < 400\mu s$. So, the two dips appear around $t = 200\mu s$ and $t = 600\mu s$ for $F_{dd} = 5kHz$. In the case where a CPMG π-pulse sequence with $F_{dd} = 10kHz$ is applied, the first π-pulse is applied at $t = 100\mu s$ and the second π-pulse is applied at $t = 300\mu s$, … . In this case, the CPMG π-pulse sequence can timely protect the qubit memory from decoherence and then the quantum process fidelity keeps a slow monotonous decrease with the storage time *t*. At 800μs, the quantum process fidelities reach ~80% for the cases of $F_{dd} = 5kHz$ and $F_{dd} = 10kHz$. Figure 6 shows the quantum process fidelity at storage time of 800μs as the function of the π-pulse number *n* (lower) and the frequency F_{dd} (upper), respectively. The measured quantum process fidelity is better than 0.8 for $n = 4$ and 0.77 for $n = 6$.

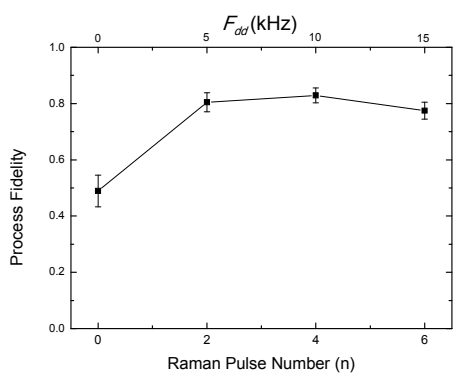

Fig. 6. Quantum process fidelity F_p at storage time of 800μs as the function of the number of π-pulses *n* (lower) and the frequency F_{dd} (upper).

4. Discussions

We perform the polarization quantum memory with the classical signal-light pulses of different polarization. However, our storage scheme will also hold for the single-photon polarization states because the attenuation of the signal light in the storage process is linear [28] [29] [30]. In other words, the measured polarization fidelities for the single photons will be close to that for the classical light pulses. However, there might exist the background noise photons directed into the single-photon detectors, which will degrade the quantum fidelity of the single-photon polarization states. The background photons may come from the leakage

#216479 - $15.00 USD Received 7 Jul 2014; revised 17 Aug 2014; accepted 1 Sep 2014; published 17 Sep 2014
(C) 2014 OSA

photons from reading beam or spontaneous emissions from the atomic ensemble. For blocking the leakage photons from the reading beam, we may insert more number of optical filters before single-photon detectors. The reason for the generation of the spontaneous emissions is explained in the following. In the atomic ensemble, there may exist small number of atoms which are in the excited state $|b\rangle$ but are not associated with the spin waves. When the reading beam is switched on to drive the transition $|b\rangle \leftrightarrow |e\rangle$, these atoms will be excited to $|e\rangle$ and then generate spontaneous emissions. Many processes, for example, thermally excitations, etc., may induce incoherently transfer from the state $|a\rangle$ into the state $|b\rangle$. In the presented scheme, the Raman π-rotations is one process which induce incoherently transfer from the state $|a\rangle$ into $|b\rangle$ [26]. By taking large enough detuning Δ_R (Δ'_R) of Raman laser from the transition $|b\rangle \leftrightarrow |e\rangle$ ($|b\rangle \leftrightarrow |5P_{1/2}, F'=2\rangle$, the number of the transferred atoms will be decreased [26] and then the background noise photons coming from such process may be significantly suppressed.

5. Conclusions

We demonstrate PPQ's storages protected by CPMG DD sequences. The process fidelity better than 0.8 is measured for up to 800μs storage time with a $10kHz$-frequency CPMG sequence being applied, while, it is measured for up to 180μs storage time without CPMG sequence. Compared with the previously reported PPQ's storages [12,13], an advantage of the presented long-lived PPQ's storage is that single-qubit operations can be easily implemented during storage. We believe that this advantage can be used to improve the success probability of the quantum teleportation based on atomic ensembles [31] and find more effective applications in quantum information processing.

Acknowledgments

We acknowledge funding support from the 973 Program (2010CB923103), the National Natural Science Foundation of China (No.10874106, 60821004).